



# 3D Vector Approach to Local Thermally Driven Slope Winds Modeling

Alfonso Vitti\*, Paolo Zatelli<sup>#</sup> and Fabio Zottele<sup>+</sup>

Department of Civil and Environmental Engineering  
via Mesiano 77, 38100 Trento, Italy

\* Tel: +390461882608 Fax: +390461882672 E-mail: alfonso.vitti@ing.unitn.it

<sup>#</sup> Tel: +390461882618 Fax: +390461882672 E-mail: paolo.zatelli@ing.unitn.it

<sup>+</sup> Tel: +390461882618 Fax: +390461882672 E-mail: fabio\_zottele@hotmail.com

## Abstract

*A vector model has been setup to evaluate wind velocity and direction for thermally driven slope winds. This model is based on an extension of the Prandtl model and uses the new GRASS 3D vector implementation as well as its connection to external DBMS. This model follows a previous raster approach for the implementation of a local meteorological model based on the 3D raster GRASS capability. The new vector implementation allows the evaluation of temperature, wind velocity and direction on a set of irregular placed points, while the raster approach is constrained to use points on a regular grid. Moreover, all the attributes that are used as parameters in the model are managed through SQL statements. A new algorithm has been developed to evaluate the normal direction through a point in the 3D space, since all the model parameters depend on the distance from the surface along the normal direction. A comparison between the vector and the raster approach, in terms of implementation and use, is presented. Finally a synthetic and a real simulation and a comparison with the raster model results are reported.*

## 1. Introduction

The integration of environmental models and GIS is driven by the effort towards the development of a comprehensive description of a system, where each interrelated factor can be correlated by its position in the space. In fact, the management of heterogeneous data linked by their position is what GISs are about.

The development of a model for local atmospheric study within a GIS environment has started some years ago, resulting in a local thermally driven slope winds model based on the 3D raster GRASS model (Ciolli et al., 2004; Ciolli et al., 2002a; Ciolli et al., 2002b). This model evaluates wind velocity and potential temperature anomaly in a volume over a slope.

The raster approach implies that, while it is possible to choose the resolution along the three

axes, the variables must be estimated over the whole domain. Since heavy geometric calculation is involved for the determination of the normal direction to the terrain surface, this can be needless burdensome when the values in only a small set of point are needed. For example the model has been tested matching its output against the measurement taken by a motor glide in the Adige valley, about 2 km wide, with an entire track about 15 km long and 2 km high (de Franceschi et al., 2003). The total air volume involved in the measurements is about 60 km<sup>3</sup>, therefore a discretisation with 10×10×10 m<sup>3</sup> voxels implies 60 millions of cells.

A vector approach, where wind velocity and potential temperature anomaly can be evaluated on an arbitrary set of points, makes the matching between simulated and measured

values feasible since it is sufficient to perform the calculations only on the glide trajectory, which is determined by GPS.

Therefore, the first goal of this work is the implementation of all the geometric part of the model following a vector approach. Moreover, the application of the model can be made faster and more easily manageable if all the non geometric (i.e. semantic) part of the model is stored and managed by a DBMS, linked to geometric data.

## 2. Thermally Driven Slope Winds

The diurnal cycle of incoming solar radiation and outgoing longwave radiation at night determines a cyclical heating and cooling of the air layers closer to the ground, causing airflows along sloping terrains. These slope winds are more relevant in mountain valleys, where the temperature gradients due to the mountain slopes influence the lower air layers and the whole air motion inside a valley is affected (Whiteman, 1990).

The theoretical formulation for thermally induced flows on a slope has been provided by Prandtl (Prandtl, 1942), confirmed by the sperimental work of Defant (Defant, 1949). A sloping ground is modeled by a tilted plane, with an angle  $\alpha$  with respect to the horizontal, while the atmosphere above is unperturbed and stable. Two reference frames are usually established: one is the usual Cartesian reference, with the direction  $x$  along the slope on the horizontal plane and  $z$  in the vertical direction, the second one has a coordinate  $s$  along the slope and  $n$  normal to it.

Air movements and temperature distribution are due to the heat fluxes the air volume is exposed to. The main energy source is the solar radiation, this energy is partly reflected back to the air by the terrain surface and partly adsorbed by the ground; this latter part is in turn divided in heat flux into the ground and sensible and latent heat flux conveyed back to the air layers closer to the surface.

Indicating as positive the heat fluxes from the ground to the atmosphere, the heat budget can be written as

$$-Q_S^* = Q_H + Q_E - Q_G \quad \text{Equation 1}$$

where  $Q_S^*$  is the net solar radiation flux,  $Q_H$  the sensible heat flux,  $Q_E$  the latent heat flux and  $Q_G$  the ground heat flux. The incoming net radiation flux  $Q_S^*$  is evaluated as a fraction of the extraterrestrial solar radiance, taking into account reflection and absorption by the atmosphere, and the ground flux  $Q_G$  is estimated as a fraction of the net radiation flux  $Q_S^*$  by

$$Q_G = aQ_S^* \quad \text{Equation 2}$$

where the coefficient  $a$  ranges from 0.1 for the daytime to 0.5 for the night time. Sensible heat flux and latent heat flux are estimated by closing the budget equation, after having chosen a proper ratio between the two, the so called Bowen ratio coefficient  $\beta_R$

$$\beta_R = \frac{Q_H}{Q_E} \quad \text{Equation 3}$$

A more detailed discussion of the determination of these heat fluxes can be found in (Ciolli et al., 2004; Ciolli et al., 2002a; Ciolli et al., 2002b; Iqbal, 1983), where references are provided.

The evaluation of the the sensible heat flux  $Q_H$  is essential for the estimation of temperature and wind velocity over the slope. Rather than to absolute temperature, heat exchange is related to *potential temperature*, that is the temperature an air parcel volume would have if led to a reference pressure (usually 1000 hPa) along an adiabatic transformation. The link between absolute  $T$  and potential  $\theta$  temperature is given by the well known Poisson equation

$$\theta = T \left( \frac{P_0}{P} \right)^{\frac{R_d}{cp}} \quad \text{Equation 4}$$

where  $p$  is the atmospheric pressure,  $p_0$  is the reference pressure,  $R_d = 287 \text{ JK}^{-1}\text{kg}^{-1}$  is the gas constant for dry air and  $cp = 1004 \text{ JK}^{-1}\text{kg}^{-1}$  is the specific heat at constant pressure. Heating and cooling of the ground impart an anomaly  $\Delta\theta$  on the potential temperature, which in an unperturbed atmosphere shows a positive gradient

$$\theta = A + \Gamma z + \Delta\theta(n) \quad \text{Equation 5}$$

where  $z$  is the vertical coordinate and  $n$  the normal coordinate to the slope,  $\Gamma$  is the potential temperature vertical gradient in standard atmospheric conditions and  $A$  an integration constant (i.e. the temperature at soil level). The anomaly of potential temperature  $\Delta\theta$  can be written as

$$\Delta\theta = Ce^{-\frac{n}{l} \cos\left(\frac{n}{l}\right)} \quad \text{Equation 6}$$

where  $C$  is the potential temperature anomaly at ground level, and  $l$  is the typical length scale of the phenomenon

$$l = 4\sqrt{\frac{4v_H v_k}{g\beta\Gamma \sin \alpha}} \quad \text{Equation 7}$$

where, again,  $v_H$  is the air thermal diffusivity,  $v_k$  is the air kinematic viscosity,  $g$  the gravity acceleration,  $\beta = 273.15^{-1}$  and  $\alpha$  the slope angle.

These same parameters can be used to estimate the wind velocity component along the slope

$$u = C\sqrt{\frac{g\beta v_H}{\Gamma v_k}} e^{-\frac{n}{l}} \sin\left(\frac{n}{l}\right). \quad \text{Equation 8}$$

The value of the integration constant  $C$  can be evaluated by imposing the boundary condition at the ground-atmosphere interface that the potential temperature variation in the  $n$  direction is proportional to the sensible heat flux  $Q_H$ . On the basis of the Fourier law it is possible to write

$$Q_H = -k_H \frac{\partial \Delta\theta}{\partial n} \Big|_{n=0} \quad \text{Equation 9}$$

where  $k_H$  is the air thermal conductivity; the potential temperature anomaly variation along the  $s$  coordinate can be neglected considering the motion as uniform along the slope. By substituting Equation 6 in 9,  $C$  can be expressed as

$$C = \frac{Q_H l}{k_H}. \quad \text{Equation 10}$$

It is possible to take into account the effects of water vapor, modifying the Prandtl model, by introducing the virtual potential temperature  $\theta_v$

$$\theta_v = (1 + 0.61q)T \left( \frac{P_0}{P} \right)^{\frac{R_d}{cp}} = \theta (1 + 0.61q) \quad \text{Equation 11}$$

where  $q$  is the specific humidity. The expressions for  $\theta_v$  and  $u$  can be derived by applying the same procedure above, but in addition to the heat budget condition of equation 1 the conservation of moisture flux must be imposed (Ciolli et al., 2002a).

### 3. GIS Procedure

As seen in the previous section, the evaluation of potential temperature anomaly and wind velocity along a slope requires the knowledge of the sensible heat flux on the surface and of the distance of the point from the surface itself, along the normal direction.

The sensible heat flux can be evaluated from the incidence angle between solar beams direction and the normal to the surface, the atmosphere features and the land cover. The incidence angle can be determined by a program for the computation of the solar radiation. The relevant atmospheric parameters are the absorption, reflection and transmission coefficients, the atmospheric transmissivity and the cloud cover factor. The land cover influence is taken into account by the albedo, soil thermal capacity and, for vegetation cover, leaf resistance to vapor flux. All these parameters must be available as geographically

referenced information, so that their combination to evaluate the sensible heat flux is possible. In the raster approach each parameter is represented by a raster 2D map on the terrain or a set of atmospheric parameters, in the vector approach the parameters are stored in a database and linked dynamically to the vector geometry. The only raster map, required by the vector model, is the digital terrain model (DTM), but a vector DTM such as a TIN can be used.

#### 4. Evaluation of the Normal to a Surface

The terrain surface is expressed by a raster DTM and slope and aspect maps are easily evaluated. While the gradient components of the DTM would be more suitable for the determination of the normal direction though a point in the space, the wide availability of slope and aspect information makes these parameters preferable for this task.

The main problem in the individuation of the normal to a DTM through a point is that in general a DTM does not describe a simple geometric known surface, therefore it is not possible to write an explicit expression for the normal direction. The workaround comes from the observation that for points close to the surface the distance on the surface between their *normal* and *vertical* projection is usually small, save for singular situations. The determination of the vertical projection on the surface is trivial and this point can be used as starting point for the search of the normal projection, which is the point corresponding to the minimum distance. The algorithm that evaluates the normal to a surface uses this proposition, starting from a point close to the surface and moving towards the interesting point.

Let  $P(x_p, y_p, z_p)$  be the point to be projected and  $V(x_v, y_v, z_v)$  its vertical projection on the surface, the segment  $\overline{PV}$  is divided into  $k$  parts, each with edge points  $P_v(i)$  with coordinates:

$$\left( x_p - i \frac{\overline{PV}}{k}, y_p - i \frac{\overline{PV}}{k}, z_p - i \frac{\overline{PV}}{k} \right) \text{ with } i$$

running from 0 to  $k$ , where obviously  $P_v(i) \equiv V$  for  $i=0$ ,  $P_v(i) \equiv P$  for  $i=k$  and lower values of  $k$  correspond to points closer to the surface. The algorithm starts with  $k=1$ ; for this point  $P_v(1)$ , which is close to the terrain surface, the normal and vertical direction are close, unless the slope is very slanting or a singularity of the surface is involved. Therefore, a window of points under  $P_v(1)$  is scanned and the distances from  $P_v(1)$  to the centers of all these cells are evaluated. Then the point  $Q(x_Q, y_Q, z_Q)$  corresponding to the shortest distance  $d_{min} = \overline{PQ}$  is selected.

The versor

$$\vec{v}_Q = \frac{\overline{Q - P_v(1)}}{d_{min}} \quad \text{Equation 12}$$

identifies the direction of the segment from  $P_v(1)$  to  $Q$ , which in general is not the normal direction since only the cell centers are tested. Still, it is possible to evaluate the normal direction to the terrain surface from the DTM gradient for the cell to which  $Q$  belongs. This is done by calculating the versor

$$\vec{v}_{DTM} = \frac{\vec{\nabla}}{\|\vec{\nabla}\|} = \frac{(\nabla_x, \nabla_y, \nabla_z)}{\sqrt{(\nabla_x^2 + \nabla_y^2 + \nabla_z^2)}} \quad \text{Equation 13}$$

If  $\vec{v}_Q = \vec{v}_{DTM}$  then  $\vec{v}_Q$  is the normal direction through  $P_v(1)$ , otherwise, as usually happens, the distance from  $Q$  to the normal projection point  $N(x_N, y_N, z_N)$  can be evaluated as follows

$$d = |\vec{v}_Q \cdot \vec{v}_{DTM}| \|P - Q\| \quad \text{Equation 14}$$

and  $N$  is found by moving of  $d$  along the opposite direction of  $\vec{v}_{DTM}$

$$N = P - \vec{v}_{DTM} d \quad \text{Equation 15}$$

Once the projection point  $N$  for  $P$  is found, the procedure is iterated for the other  $k-1$  points. However, after the first iteration the point  $N$  of the previous iteration, rather than the vertical projection, is used as starting point for the search.



The two parameters that must be chosen in this procedure are  $k$ , the number of segments into which the vertical segment from the point to the surface is divided, and  $m$ , the dimension, as number of cells in its side, of the square search window on the terrain. These parameters are set as a trade off between the risk of selecting the wrong point on the surface and the computational cost. In fact, the choice of large values for  $k$  increases the number of iterations of the procedure above, while small values of  $k$  can lead to situations in which the hypothesis that normal and vertical directions are close does not hold, resulting in the failure of the algorithm. The selection of large values of  $m$  causes the need of scanning a large number of cells when looking for the distance minimum (the number of scanned cells scales with  $m^2$ ), however a small value of  $m$  can lead to the individuation of a *local* minimum for the cells' centers - point distance which is not the real minimum, resulting again in a failure of the procedure.

Once the coordinates of the projection point  $N$  are known, it is possible to evaluate the distance of a point from the surface along the normal direction, i.e. to calculate the  $n$  coordinate of Section 2. Moreover, the address of the cell under the point in the normal direction is known, therefore the sensible heat flux can be evaluated.

## 5. Implementation

The algorithm described in Section 4 has been implemented as a new GRASS module that creates a tridimensional vector map of the segments connecting each input point with its projection on a DTM. To each segment a record is associated, storing the following information: the coordinates of the point to be projected, the coordinates of the projection point, the distance between these points, the indexes of the DTM cell containing the projection point and the coordinates of the baricenter of the cell. This module has been written to implement a model of local thermally driven slope winds, however

it as been designed with a more generic use in mind: it solves the geometric part of the problem with no reference to the atmospheric model. For example, it is possible to evaluate the normal direction to a surface for points *below* the surface: while it makes no sense for the implementation of an atmospheric model, this can be used in other applications.

The input of the module consists of a vector map containing the points whose normal must be evaluated and three raster maps representing the DTM, the slope (in degrees) and the aspect (in degrees), the latter two are used to evaluate the local gradient of the surface. For complex (concave) terrain morphologies it is possible that more than one normal exists; the module selects the direction corresponding to the shortest distance, since the variables (temperature and wind velocity in our model) in one point are likely influenced more from closer points on the surface.

## 6. Tests and Applications

The correct functioning of the module has been checked with several test configurations. As a first set of tests, some planes have been used to match the result of the use of the module against the analytical determination of the coordinates of the projection points and their distances from the projecting point. The differences are very small and can be ascribed to numerical roundoff (Vitti et al., 2004) for the analytical details. Other experiments have been carried out for more complex surfaces such those used with the raster approach (Ciolli et al., 2004.; 2002a; 2002b). One example is depicted in Figure 1. All the points in the volume above the surface have been projected, so that the comparison with the results of the 3D raster model is possible. For every surface the results are identical, it is therefore possible to assert the good functioning of the module.

The first application is used as an overall test of the model. In fact, Defant's conditions (Defant, 1949) have been used to evaluate parameters that are matched against his sperimental



data. According to Defant's measurement campaign the following conditions are chosen: planar slope, uniform solar coverage and solar radiation, unperturbed and stratified atmosphere. The values of the constants and parameters used to solve Equations 6 and 8 can be found in Vitti et al. (2004).

Since the  $C$  parameter values reported in Vitti, Zatelli and Zottele (2004) are valid only for the initial hours of the day or of the night, a new procedure has been setup for the evaluation of the  $C$  parameter on the slope, which uses the equations of Section 2. The output of this procedure is a 2D map of the value of  $C$  for a given hour of the day. Since the successive elaboration is made by manipulating database tables, this raster map is exported as a vector map with an associated table.

The wind velocity along the slope  $u$  and the potential temperature anomaly  $\Delta\theta$  are evaluated with the following procedure:

- for each point the normal direction to the DTM surface is evaluated;
- for each point the value of  $C$  is read from the database table;
- Equations 6 and 8 are solved using a SQL statement;
- the resulting table is associated to the input vector file containing the investigated points, replacing the original table.

All the database management is done using PostgreSQL allowing great flexibility. The SQL statement solving Equations 6 and 8 are reported in Vitti et al. (2004).

The results of the application of the model match the experimental measurements in Defant (1949), the outline of the temperature distribution in case of up-slope wind and down-slope wind conditions is shown in Figure 2. Other applications have been carried out for real slopes near the city of Trento. The output of the model for a slope near the village of Besenello, 10 km south Trento along the Adige valley, Italy, are shown in Figure 3.

The same slope has been investigated in Ciolli et al. (2004; 2002a; 2002b) with a raster

approach: the comparison of the results in Figure 4 shows a good agreement between the two solutions.

## 7. Vector vs Raster Approach

The comparison of raster and vector approaches can be done in terms of overall performance of the procedure, taking into account elaboration times, ease of data management and flexibility.

The performance comparison between raster and vector approaches with respect to computational weight for the determination of the parameters on a regular domain awards the raster approach, since the higher computational cost is associated to the determination of the projection point on the surface though the point along its normal direction. In fact, the raster approach allows to store in memory the result of the adjoining cell, which can be used as start point for the search on the next voxel. The assumption that two successive points during the elaboration are near does not hold for the vector approach: it is therefore unavoidable to start with wider "search window" (see Section 4). This results in longer elaboration times and higher memory demand.

On the other hand the vector approach, with DBMS attribute management, allows great flexibility in the definition and manipulation of attribute and geometry. Attribute management benefits from all the tools available using a DBMS, since both input and output of the model can be fully expressed as database tables. Geometry flexibility is the most evident advantage of the vector model, allowing the evaluation of the parameters in a single point or on irregular sets of point. A typical choice is the use of irregular grids of points, with more dense points near the terrain surface and more sparse points far from it.

In conclusion, for regular domains the raster approach, shows a better computational performance, while for irregular set of points, or if attributes are stored in a database, the vector approach is a better choice.

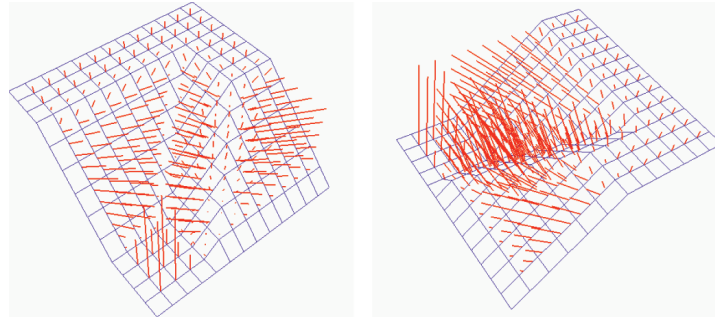


Figure 1: Two views of a synthetic DTM and of the normal segments from the centers of a regular set of points above the surface

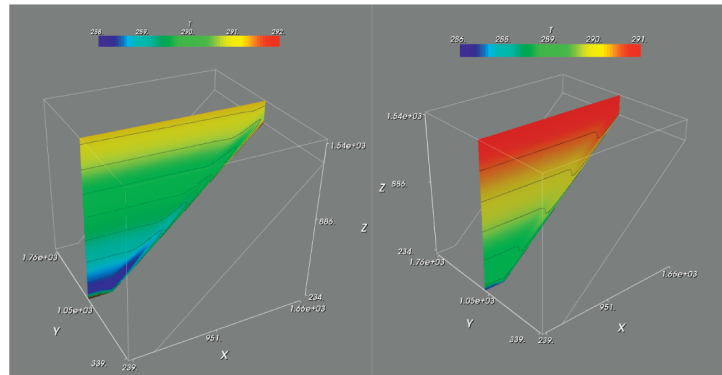


Figure 2: Output of the model for the Defant's parameters set: up-slope wind (left) and down-slope wind (right) temperature [K] distribution along the slope

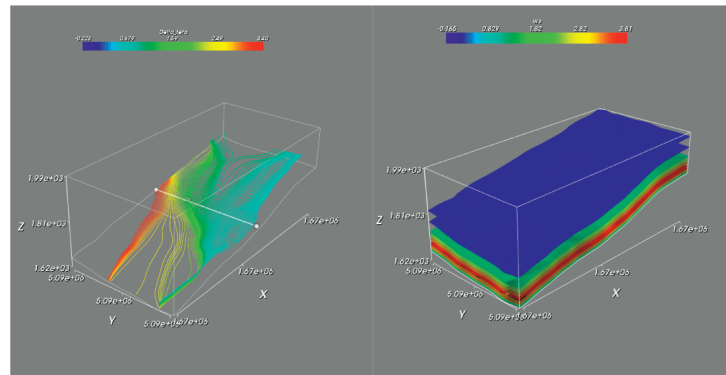


Figure 3: Potential temperature anomaly [K] distribution on the slope during the up-slope wind conditions (left) and wind velocity along the slope (here indicated as "ws") during the up-slope wind (right). Besenello (TN), Italy

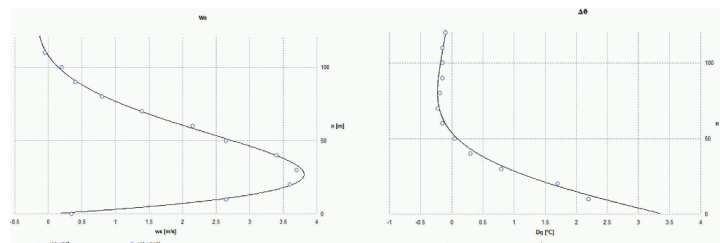


Figure 4: Comparison of the wind velocity along the slope (here indicated as 'ws') during the up-slope wind conditions for the vector (ws\_vector) and raster (ws\_voxel) approach (left) and comparison of the potential temperature anomaly [K] along the slope during the up-slope wind conditions for the vector (vect) and raster (voxel) approach. Besenello (TN), Italy



## 8. Conclusions

The new vector model, its implementation and database connection constitute a powerful environment for the setup of physical models in 3D domains. The choice between vector and raster approach depends on the model and on the geometry involved, as seen on Section 7. The value added by the development of a local atmospheric model in a GIS context lies in the availability of a proper environment for the management of referenced information and in the possibility of integrating the model's results in a broader environmental model.

The future developments of the atmospheric model include the evaluation of other parameters and a more sophisticated modeling of the influence of the land cover on sensible heat fluxes.

From the GIS point of view, apart from a general optimization of the algorithms, the attribute management through a DBMS still needs some work and the whole procedure must be made automatic though scripting to make the model accessible to non GIS specialists.

## References

- Ciolfi, M., de Franceschi, M., Rea, R., Vitti, A., Zardi, D. and Zatelli, P., 2004, Development and Application of 2D and 3D GRASS Modules for Simulation of Thermally Driven Slope Winds, *Transactions in GIS*, 8(2), 191-209.
- Ciolfi, M., de Franceschi, M., Rea, R., Zardi, D. and Zatelli, P., 2002a, Modeling of Evaporation Processes Over Tilted Slopes by Means of 3D GRASS Raster, *Proceedings Open Source Free Software GIS - GRASS users conference 2002*, Edited by M. Ciolfi and P. Zatelli, Trento, Italy, <http://www.ing.unitn.it/~grass/conferences/GRASS2002>.
- Ciolfi, M., Vitti, A., Zardi, D. and Zatelli, P., 2002b, 2D/3D GRASS Modules Use and Development for Atmospheric Modeling. *Proceedings Open Source Free Software GIS - GRASS users conference 2002*, Edited by M. Ciolfi and P. Zatelli, Trento, Italy <http://www.ing.unitn.it/~grass/conferences/GRASS2002>.
- de Franceschi, M., Rampanelli, G., Sguerso, D., Zardi, D. and Zatelli, P., 2003, Development of a Measurement Platform on a Light Airplane and Analysis of Airborne Measurements in the Atmospheric Boundary Layer. *Annals of geophysics*, 46(2), 269-283.
- Defant, F., 1949, Zur Theorie der Hangwinde, nebst Bemerkungen zur Theorie der Berg- und Talwinde, *Archiv fuer Meteorologie, Geophysik und Bioklimatologie*, A, 1, 421-450.
- Prandtl, L., 1942, *Fuehrer durch die Stroomungslehre*. Braunschweig. Vieweg und Sohn.
- Whiteman, C. D., 1990, Observation of Thermally Developed Wind Systems in Mountain Terrain Atmospheric Processes over Complex Terrain. In *Atmospheric Processes over Complex Terrain*, Edited by W. Blumen. Washington, D.C., American Meteorology Society Monograph No. 23, 5-42.
- Iqbal, M., 1983, *An introduction to solar radiation*. (New York: Academic Press).
- Vitti, A., Zatelli, P. and Zottele, F., 2004, 3D Vector Approach to Local Thermally Driven Slope Winds Modeling, *Proceedings Free/Libre and Open Source Software (FOSS) for Geoinformatics: GIS-GRASS Users Conference*, Edited by P. Santitamnont and V. Raghavan, Chulalongkorn University, Bangkok, Thailand, in CD Rom.